Image Contrast Enhancement based Combined Techniques without Over-enhanced Noise

I. A. Humied[1], F. E. Z. Abou-Chadi[2], M. Z. Rashad[3]

Faculty of Computers and Information Sciences, Mansoura University, Mansoura, Egypt

Abstract

In order to enhance the contrast noisy images where the amplitudes of it histogram components are very high at one location on the gray scale and very small in the rest of the gray scale, conventional global contrast enhancement schemes over-equalize these images so that too bright or dark pixels are resulted and local contrast enhancement schemes produce unexpected discontinuities at the boundaries of the blocks or not fully automated. A new combined technique was presented for contrast enhancement these images. The new combined technique segments the original histogram into tow sub-histograms with reference to the location of the highest amplitude of the histogram components and equalizes the left sub-histogram using Histogram Equalization (HE) and the right using Fast Gray Level Grouping (FGLG). The final image is determined as the sum of the equalized images obtained by using the sub-histogram equalizations and the over-equalization effect is eliminated. Also the result image does not miss feature information in low density histogram region since it applied separating equalization. In the present paper, the effect of noise on the performance of this technique is investigated.

Keywords:

Contrast Enhancement, Histogram Equalization, Fast Gray-Level Grouping, Equalization Noisy Images.

I. Introduction

Because some features are hardly detectable by eye in an image, we often transform images before display. Numerous contrast enhancement techniques exist in literature, such as gray-level transformation based techniques (e.g., logarithm transformation, power-law transformation, piecewise-linear transformation, etc.) and histogram processing techniques (e.g., histogram equalization (HE), histogram specification, etc.) [1].

Histogram equalization (HE) is one the most well-known methods for contrast enhancement. Such an approach is generally useful for images with poor intensity distribution. Its basic idea lies on mapping the intensity levels based on the probability distribution of the input intensity levels. It flattens and stretches the dynamics range of the image's histogram and resulting in overall contrast improvement [2]. However, it tends to change the brightness of an image and hence, often fail to produce satisfactory results for a broad variety of low-contrast images. Such as, the original image have the amplitudes of its histogram components are very high in the first component of the nonzero histogram components *NZHC*, e.g., at the zero location on the gray scale and very small in the rest of the gray scale, which could cause a washed-out effect on the appearance of the output image [3].

Recently, a histogram-based optimized contrast enhancement technique called gray-level grouping (GLG) was developed by Chen et al. [3]. The basic procedure of this technique is to first group the histogram components of a low-contrast image into a proper number of groups according to a certain criterion, then redistribute these groups of histogram components uniformly over the grayscale so that each group occupies a grayscale segment of the same size as the other groups, and finally ungroup the previously grouped gray-levels.

To reduce time in GLG technique as well as the number of iterations, a default value can be used for the total number of gray-level bins, 20. In this method there is no need of constructing the transformation function and calculating the average distance between pixels on the grayscale for each set of gray-level bins. This method is called fast gray-level grouping (FGLG) since it is executed faster than basic GLG, as in [3]. It enhances the contrast of images that have the position of the highest amplitude histogram component, P_{hist}, in the first component of the nonzero histogram components *NZHC*. These techniques cannot enhance low contrast images that have P_{hist} lie in any location of the left region of *NZHC* [4]. Fig. 1 shows the flow chart of a new combined technique was presented for contrast enhancement these images [5].

Fig. 2 show the histograms of a virtual image in four basic intensity characteristics (dark, light, low contrast and high contrast) which the P_{hist}, solid line, lies in the left region of *NZHC*. The horizontal axis of each histogram plot corresponds to intensity values, r_k. The vertical axis corresponding to values of the probability of occurrence of intensity levels, $P(r_k)$.

Manuscript received July 5, 2013
Manuscript revised July 20, 2013

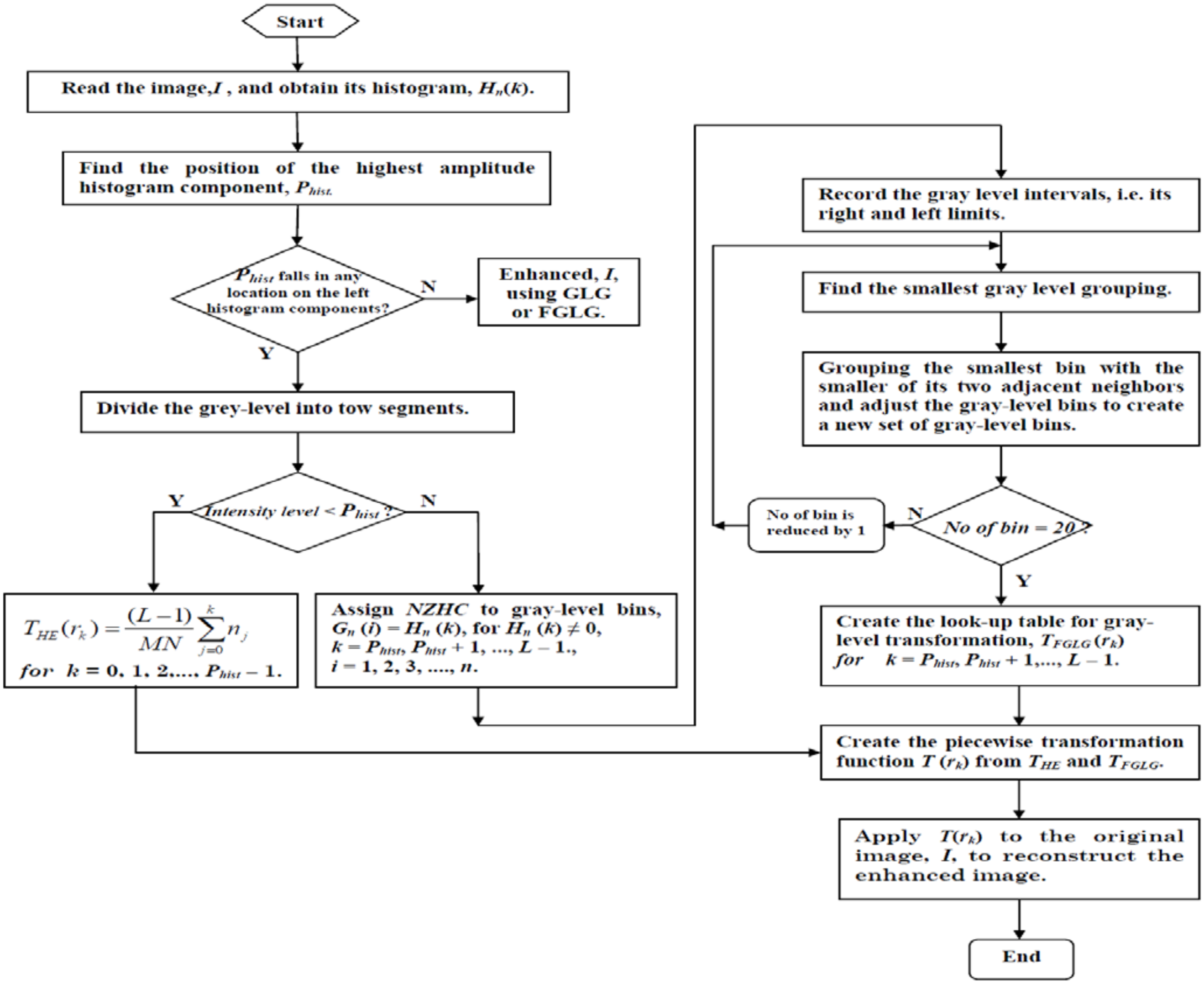

Fig. 1: Flow chart of the new combined technique algorithm with combination of HE and FGLG [5].

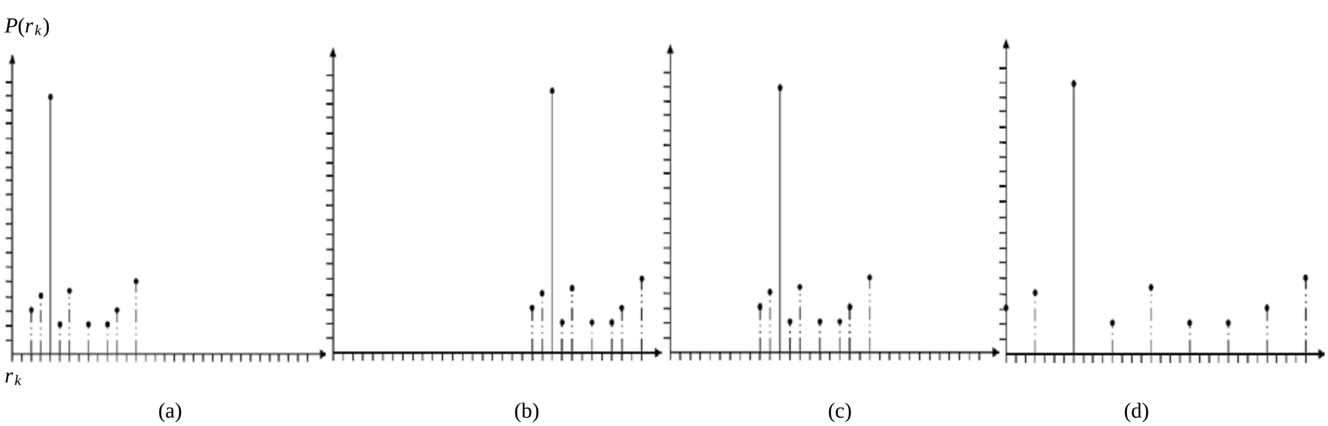

Fig. 2: Histograms of a virtual image in four basic intensity characteristics. (a) Dark image. (b) Light image. (c) Low contrast image. (d) High contrast image.

In this paper, some noise models are adding to low contrast images and observing the effect of these noises on performance of the new combined technique.

This paper is organized as follows. The new combined technique is described in the next section. Section 3 presents some important noise probability density functions. In section 4, the experimental results to testing performance the new combined technique in the presence of different noise types are presented and evaluated. Section 5 is the conclusion.

II. THE ALGORITHM OF THE NEW COMBINED TECHNIQUE

In this section, the new combined technique performs effectively with images that have the position of the highest amplitude histogram components lies in the left of *NZHC* region. It is a combination of Histogram Equalization (HE) and Fast Gray Level Grouping (FGLG). This method is carried out via various stages. Fig.1 illustrates a schematic diagram of this method [5].

The histogram of an image with intensity levels in the range [0, L – 1] is a discrete function $h(r_k) = n_k$, where r_k is the kth intensity level and n_k is the number of pixels in the image with intensity r_k. It is common practice to normalize a histogram by dividing each of its components by the total number of pixels in the image, denoted by product MN, where, as usual, M and N are the row and column dimensions of the image. Thus, a normalized histogram is given by $P(r_k) = n_k / MN$, for $k = 0, 1, 2, \ldots, L - 1$. Loosely speaking, $P(r_k)$ is an estimate of the probability of occurrence of intensity level r_k in an image. Suppose that an input image I with intensity levels in the range [0, L – 1] and its histogram was calculated, the basic procedure of the new combined technique is as follows:

A. Histogram Segmentation

Find the position of the highest amplitude histogram component, P_{hist}, on the gray scale. If P_{hist} lies inside the left segment of the *NZHC* but not in the first component of the *NZHC*, the histogram can be segmented into two sub-histograms, the first starting from 0 to (P_{hist} – 1) intensity and the second starting from P_{hist} to maximum intensity level (L – 1). On the other hand, if P_{hist} lies inside the right segment of the *NZHC* or in the first component of the *NZHC* then we have to enhance low contrast image using GLG or FGLG.

B. Piecewise Transformed Function

Having performed the histogram segmentation based on the position of the highest amplitude histogram component, P_{hist}. We can directly apply the HE to first sub-histogram from 0 to (P_{hist} – 1) and apply FGLG to second sub-histogram from P_{hist} to L – 1. The transformation function using HE can be expressed as followed [1], [2]:

$$T_{HE}(r_k) = (L-1)\sum_{j=0}^{k} p_r(r_j) = \frac{(L-1)}{MN}\sum_{j=0}^{k} n_j \qquad (1)$$

for k = 0, 1, 2,..., P_{hist} – 1. The transformation function using FGLG is $T_{FGLG}(r_k)$, for $k = P_{hist}, P_{hist} + 1, P_{hist} + 2, \ldots, L - 1$, as shown in Fig. 1. Therefore the piecewise transformed function $T(r_k)$ can be expressed as followed:

$$T(r_k) = T_{HE}(r_k) + T_{FGLG}(r_k) \qquad (2)$$

for $k = 0, 1, 2, \ldots, L - 1$. Finally, the piecewise transformed function is applied to the original image to reconstruct the optimal enhanced image.

III. SOME IMPORTANT NOISE PROBABILITY DENSITY FUNCTIONS

The spatial noise descriptor with which we shall be concerned is the statistical behavior of the intensity values in the noise component of the model in Fig 3. These may be considered random variables, z, characterized by a probability density function (PDF), $p(z)$. The following noise models are among the most common PDFs found in image processing applications [6].

A. Gaussian noise

The PDF of a Gaussian random variable, z, is given by

$$p(z) = \frac{1}{\sqrt{2\pi\sigma}} e^{-(z-z')^2/2\sigma^2} \qquad (3)$$

where z represents intensity, z` is the mean value of *z(the default value of z`is zero in this paper),* and σ is its standard deviation. The standard deviation squared, σ^2, is called the variance of z. The Gaussian image noisily and statistics of this noise, with sigma = 0.01, are show in Fig. 3(a).

B. Impulse noise

An image corrupted by impulse noise can be modeled, as described in [7]–[9]:

$$x_j = \begin{cases} c_j, \text{with probability} & 1-p \\ s_j, \text{with probability} & p \end{cases} \qquad (4)$$

Where j is the 2-D position vector, c_j is the j'th pixel value in the clean image c and s_j the pixel value in the impulse noise image s. The noise image s is usually a uniformly distributed random process with the value range of either {a, b} or [a, b], where in the first case it is commonly referred to as the salt-and-pepper noise and in the second the (continuous) random valued impulse noise. In either case, the noise variance σ^2 in the image x is expressed as $\sigma^2 = p.\alpha b^2$, where α is a constant depending on the noise type. Therefore finding the noise variance σ^2 is equivalent to finding the noise mixing probability p in (4). Figure 3(b) shows the impulse image noisily and statistics of this noise, with sigma = 0.01.

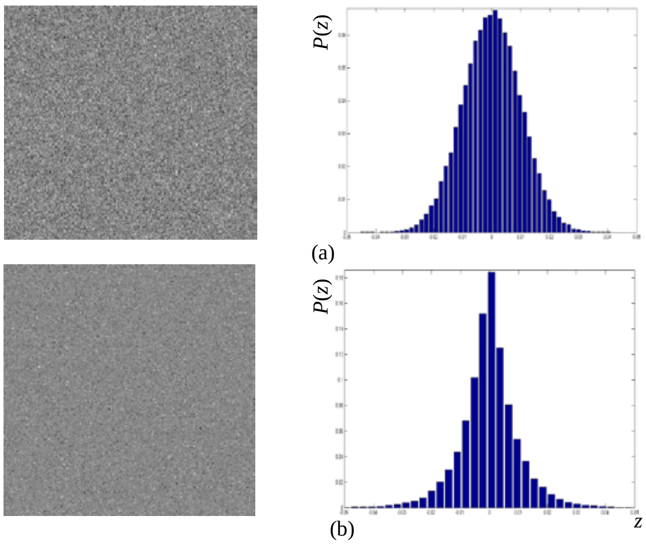

Fig. 3: The image noise models and there statistics with sigma = 0.01. (a) Gaussian. (b) Impulse.

IV. EXPERIMENTAL RESULTS

To demonstrate the effectiveness of the adding noise on the performance of the new combined technique, i.e., the noise models as we mentioned earlier are added to a variety of low contrast gray scale images and the new algorithm was applied to these images.

Fig. 4 shows the original low contrast images, with P_{hist} = 27, 13 intensity levels, and its histograms. Fig. 5 shows Fig. 4 after applied the new combined technique on it.

In addition to qualitative evaluation, quantitative measures are utilized to evaluate the performance of new combined technique. The Peak Signal-to-Noise Ratio (*PSNR*), Mean Square Error (*MSE*) and Absolute Mean Brightness Error (*AMBE*) are the most common measures for picture quality in image processing [10]. Table 1, lists the computed values, *PSNR*, *MSE* and *AMBE* values obtained from the Figs. 4 and 5.

The *PSNR* is defined as follows:

$$PSNR = 10\log_{10}\frac{255^2}{MSE} \qquad (5)$$

where *MSE* is mean-square error, defined as

$$MSE = \frac{1}{MN}\sum_{x=1}^{M}\sum_{y=1}^{N}[I(x,y)-\bar{I}(x,y)]^2 \qquad (6)$$

Where I and $\bar{I}$ are the original and enhanced image, of size $M \times N$. Note that higher *PSNR* value and lower *MSE* represents greater image quality.

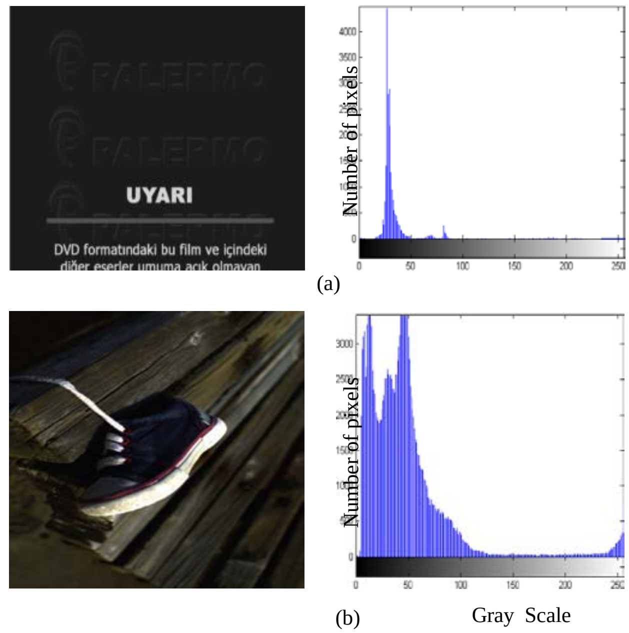

Fig. 4: The original low contrast images and its histograms with Phist equal to (a) 27 intensity level. (b) 13 intensity level.

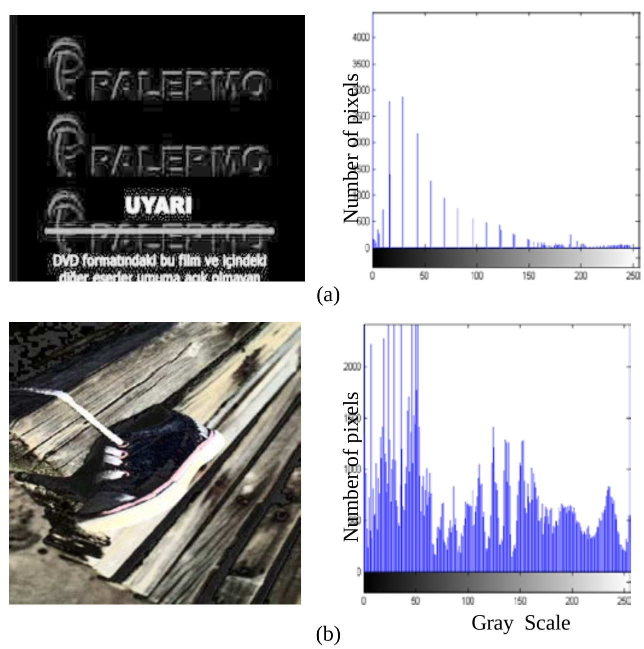

Fig. 5: Enhanced images from Fig. 4 using the new combined technique.

Table 1: The values of *PSNR*, *MSE* and *AMBE* of Figs 4 and 5.

Criterion	Images	
	a	***b***
PSNR	16.129	2.5485
MSE	1585.5	36160
AMBE	0.009	0.2438

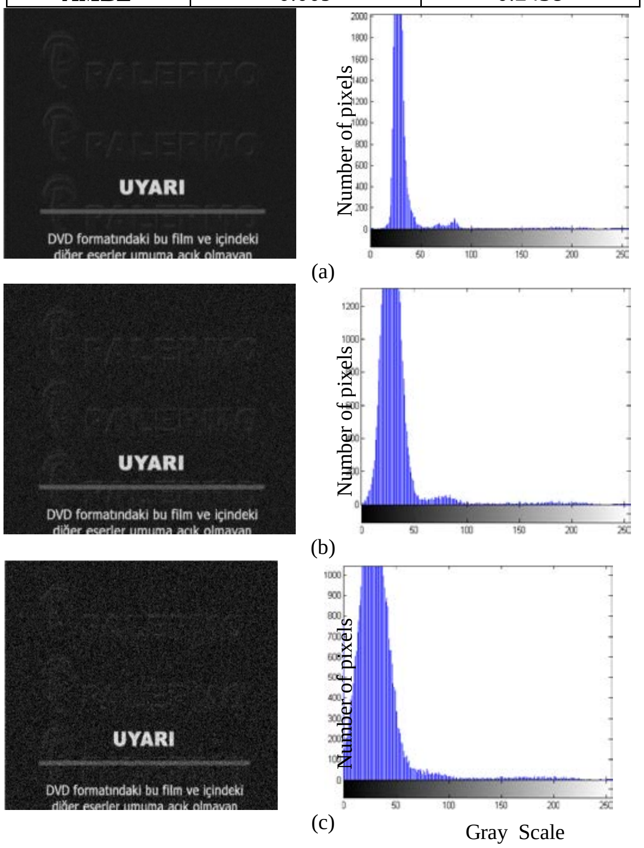

Fig. 6: The noisily images by additive Gaussian noise to Fig.4 (a). (a) σ = 0.01, (b) σ = 0.03 and (c) σ = 0.05.

The performance of brightness preservation is rated by an objective measurement *AMBE*. It is defined as the absolute differential gray-level mean between the original image and enhanced image.

$$AMBE = \left| I_m - \bar{I}_m \right| \qquad (7)$$

I_m and $\bar{I}_m$ denote the gray-level mean of the original and enhanced image. The lower *AMBE* value indicates that the brightness is better preserved and greater image quality.

Fig. 6 shows the Fig.4 (a) after adding Gaussian noise with sigma = 0.01, 0.03 and 0.05. The original image after adding this noise is changed slightly in visual but the histogram of this image is changed clear as shown in the right column of Fig.6.

Fig. 7 shows the results of applying the new combined technique on Fig. 6. It is clear that the performance of this algorithm deteriorates by increasing the value of sigma. The best performance is obtained when sigma is equal to 0.01. However, for larger sigma, the performance of the new combined technique deteriorates.

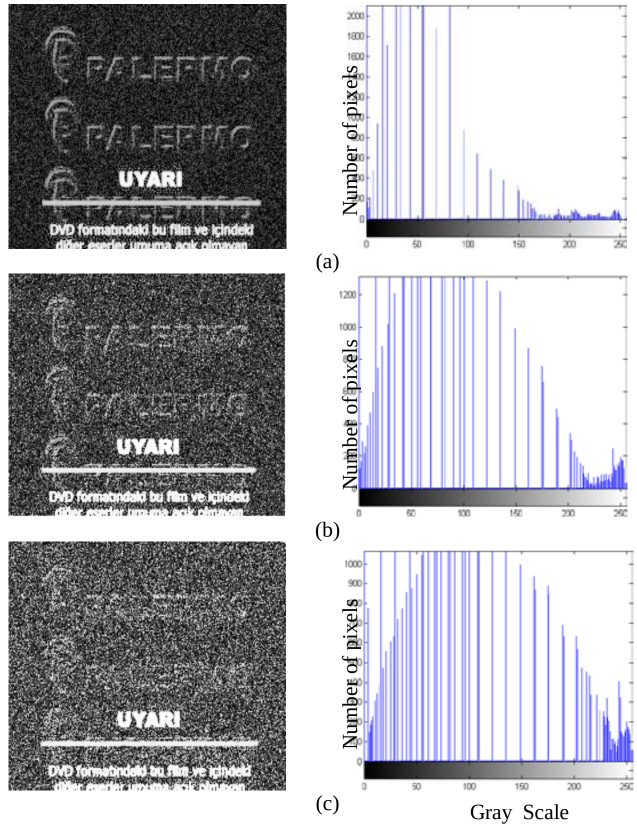

Fig. 7: Enhanced images from Fig. 6 using the new combined technique. (a) σ = 0.01, (b) σ = 0.03 and (c) σ = 0.05.

Table 2, lists the computed values, *PSNR*, *MSE* and *AMBE* values obtained from Figs. 6 and 7. From the table, it is noted that the new combined technique gives the highest *PSNR* and the lowest *MSE* and *AMBE* values for the smallest values of sigma.

Table 2: The Values of PSNR, MSE and AMBE of Figs 7 obtained using the new combined technique.

Criterion	Sigma (σ)		
	0.01	**0.03**	**0.05**
PSNR	15.1456	11.2886	9.5782
MSE	1988.5	4833.0	7165.8
AMBE	0.0907	0.1991	0.2638

Fig. 8 shows the Fig.4 (a) after adding impulse noise with sigma = 0.01, 0.03 and 0.05. The original image in visual and histogram of it after adding this noise is changed slightly.

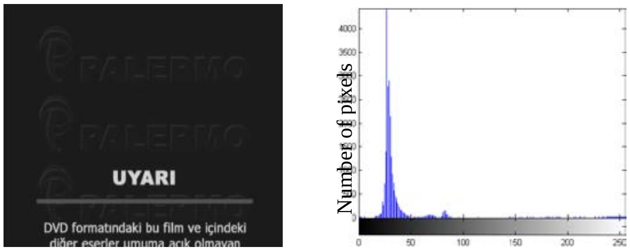

(a)

Table 3: The values of PSNR, MSE and AMBE of Fig 9.

Criterion	**Sigma (σ)**		
	0.01	**0.03**	**0.05**
PSNR	16.0793	15.7000	14.0901
MSE	1591.6	1750.2	2535.5
AMBE	0.0102	0.0521	0.1093

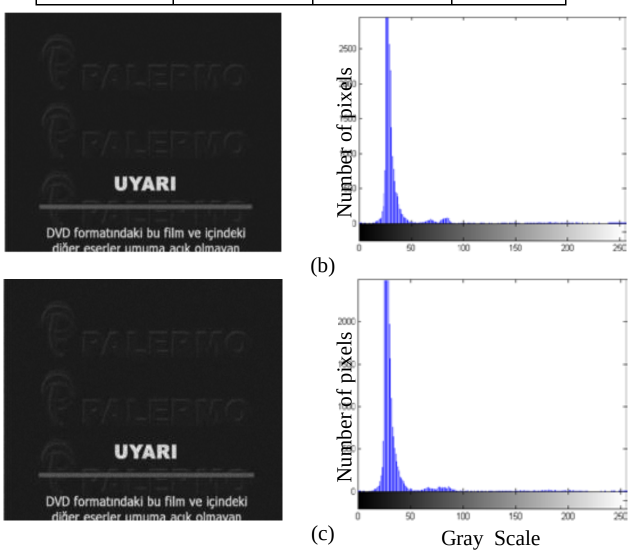

Fig. 8: The noisily images by additive impulse noise with (a) σ = 0.01, (b) σ = 0.03 and (c) σ = 0.05.

Fig. 9 shows the results of applying the new combined technique on Fig. 8. It is clear that the performance of this algorithm deteriorates by increasing the value of sigma. The best performance is obtained when sigma is equal to 0.01. However, for larger sigma, the performance of the new combined technique deteriorates but this effect is less as comparison when adding Gaussian noise on this image, as shown in Fig. 7.

Table 3, lists the computed values, *PSNR*, *MSE* and *AMBE* values obtained from Figs. 8 and 9. From the table, it is noted that the new combined technique gives the highest *PSNR* and the lowest *MSE* and *AMBE* values for the smallest values of sigma.

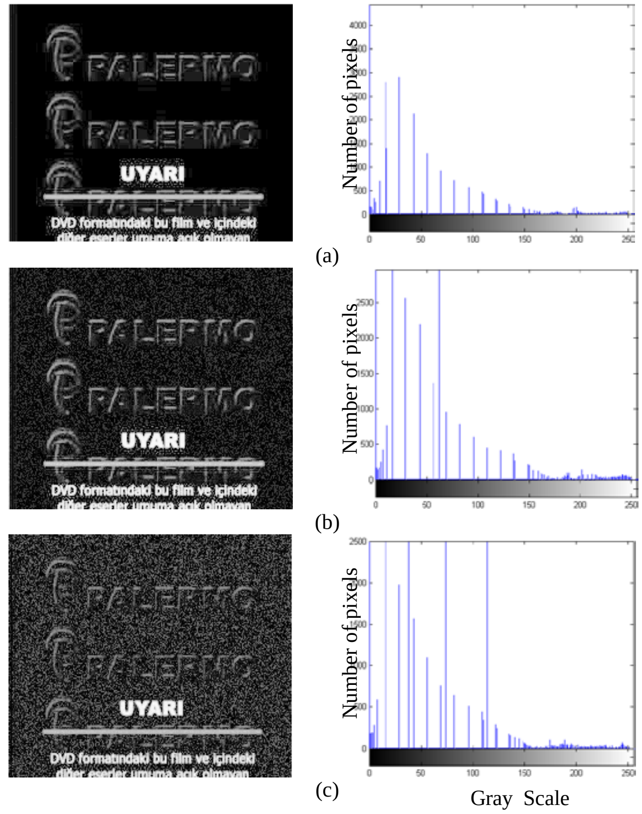

Fig. 9: Enhanced images of Fig. 8 using the new combined technique (a) σ = 0.01, (b) σ = 0.03 and (c) σ = 0.05.

Fig. 10 shows the Fig.4 (b) after adding smaller values of Gaussian noise than the previous values with sigma = 0.001, 0.003 and 0.005. The original image and histogram of it after adding this noise is changed slightly in visual. Therefore the results of applying the new combined technique on this figure are similar as shown in Fig. 11. It is clear that the performance of this algorithm not effected on these values of sigma.

The following table, table 4, lists the values of *PSNR*, *MSE* and *AMBE* values obtained from the enhancement of the images in Fig. 10 using the new combined technique (Figs. 11). These also show that the new combined technique gives the neared values of *PSNR*, *MSE* and *AMBE* for these values of sigma.

Table 4: The values of PSNR, MSE and AMBE of Fig 11.

Criterion	**Sigma (σ)**		
	0.01	**0.03**	**0.05**
PSNR	2.5197	2.3764	2.5715
MSE	36163	37622	37969
AMBE	0.2519	0.2611	0.2625

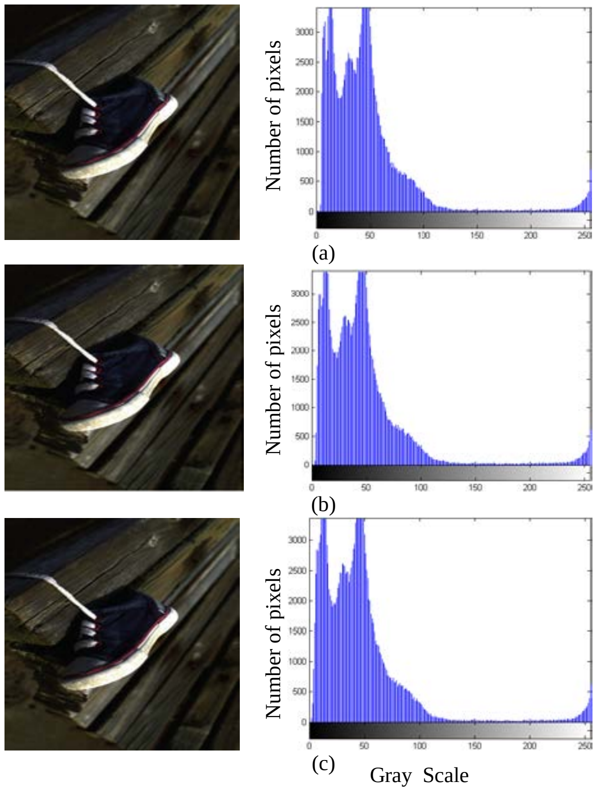

Fig. 10: The noisily images by additive Gaussian noise to Fig.4 (b). (a) σ = 0.001, (b) σ = 0.003 and (c) σ = 0.005.

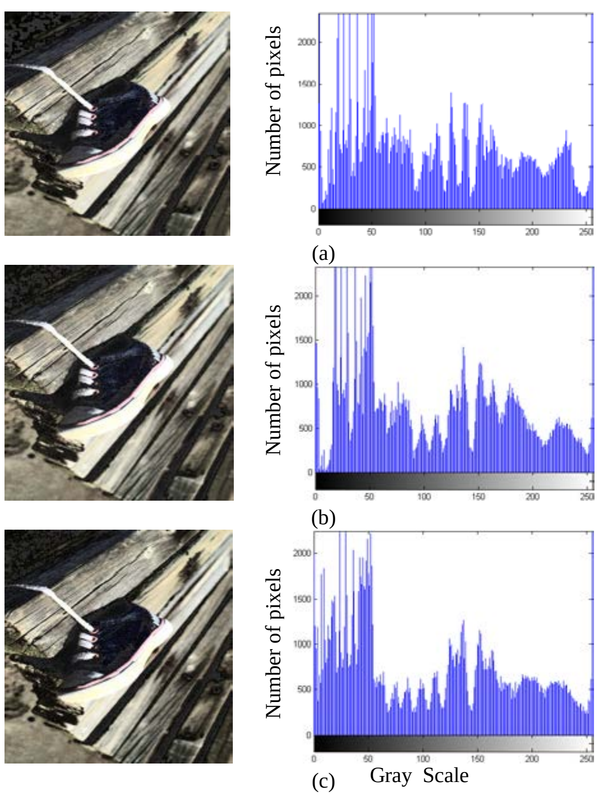

Fig. 11: Enhanced images from Fig. 10 using the new combined technique. (a) σ = 0.001, (b) σ = 0.003, (c) σ = 0.005.

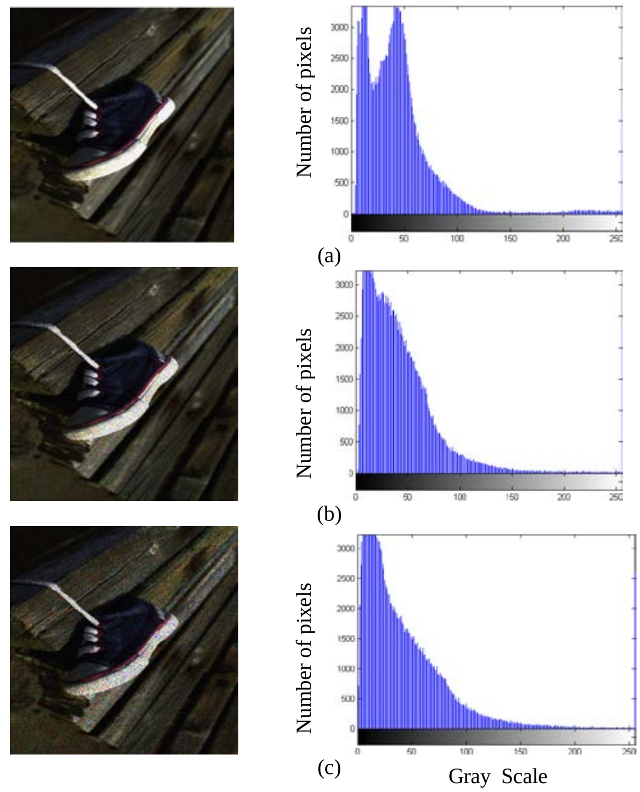

Fig. 12: The noisily images by additive impulse noise to Fig.4 (b). (a) σ = 0.001, (b) σ = 0.003 and (c) σ = 0.005.

Fig. 12 shows also the Fig.4 (b) after adding impulse noise with sigma = 0.001, 0.003 and 0.005. The original image after adding this noise is changed slightly in visual but the histogram of this image is changed clear as shown in the right column of Fig.12.

Fig. 13 shows the results of applying the new combined technique on Fig. 12. It is clear that the performance of this algorithm deteriorates by increasing the value of sigma. The best performance is obtained when sigma is equal to 0.001. Other times noted, for larger sigma, the performance of the new combined technique deteriorates.

The following table, table 5, lists the computed values, *PSNR*, *MSE* and *AMBE* values obtained from Figs. 12 and 13. From the table, it is noted that the new combined technique gives the highest *PSNR* and the lowest *MSE* and *AMBE* values for the smallest values of sigma.

Table 5: The values of PSNR, MSE and AMBE of Fig 13.

Criterion	**Sigma (σ)**		
	0.01	**0.03**	**0.05**
PSNR	2.2801	1.3784	1.3402
MSE	3846.5	4734.1	4793.6
AMBE	0.2520	0.2956	0.2404

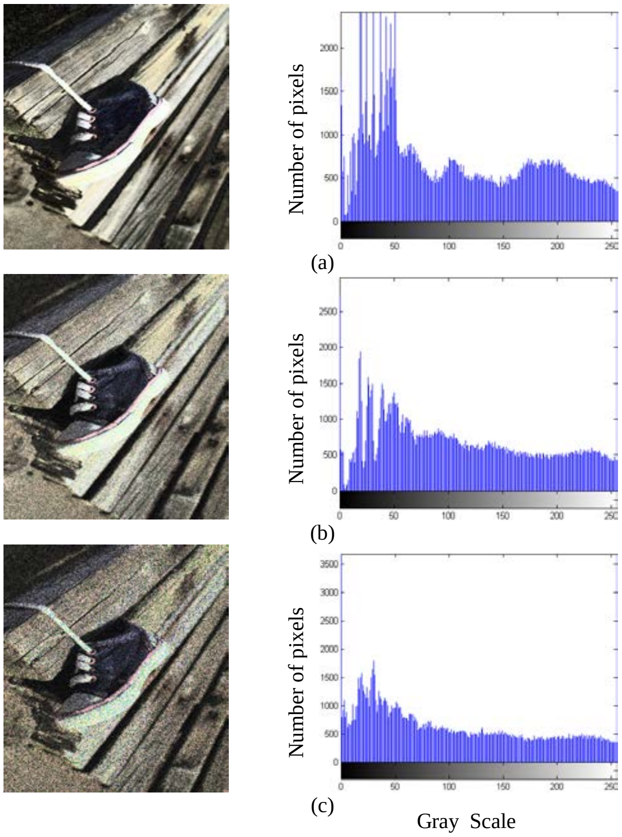

Fig. 13: Enhanced images from Fig. 12 using the new combined technique. (a) σ = 0.001, (b) σ = 0.003, (c) σ = 0.005.

It should be noted when comparison table 1 with the others tables that the new combined technique gives the highest PSNR and the lowest MSE and AMBE values for clean images. Therefore recommending eliminates the noise from the low contrast images before using the new combined technique to getting the maximum enhanced. It's also noted that all results on these tables are agreed with the visual inspection by the human eye.

V. CONCLUSION

In this paper, the general conclude that the performance of the new combined technique decreases when adding noise models (Gaussian and impulse) to low contrast images with higher noise levels. Experimental results show that the new combined technique achieves the best quality through qualitative visual inspection and the image quantitative parameters of Peak Signal-to-Noise Ratio (PSNR), Mean square error (MSE) and Absolute Mean Brightness Error (AMBE) for the clean images used. Therefore recommending eliminates the noise from the low contrast images before using this technique to getting the maximum enhanced. However, this technique can be conducted in a fully-automated manner to contrast enhancement.

References

[1] Rafael C. Gonzalez and Richard E. Woods, Digital Image Processing (3rd Edition), Prentice Hall, August 2008.

[2] William K. Pratt, Digital Image Processing: PIKS Scientific, Wiley, 2007.

[3] ZhiYu Chen, Besma R. Abidi, David L. Page, and Mongi A. Abidi, "Gray-level grouping (GLG): an automatic method for optimized image contrast enhancement-part I: the basic method," IEEE Transactions on Image Processing, vol. 15, no. 8, pp. 2290– 2302, August 2006.

[4] ZhiYu Chen, Besma R. Abidi, David L. Page, and Mongi A. Abidi, "Gray-level grouping (GLG): an automatic method for optimized image contrast enhancement-part II: The Variations," IEEE Transactions on Image Processing, vol. 15, no. 8, pp. 2303– 2314, August 2006.

[5] Ismail A. Humied, Fatma E.Z. Abou-Chadi and Magdy Z. Rashad, "A new combined technique for automatic contrast enhancement of digital images", Egypt Inform J 2012 ;13(1):27–37.

[6] http://www.mathworks.com/matlabcentral/fx_files/9554/5/content/numerical-tour/denoising_noise_models/index.html.

[7] R. H. Chan, C.-W. Ho, and M. Nikolova, "Salt-and-pepper noise removal by median-type noise detectors and detail-reserving regularization," IEEE Trans. Image Process., vol. 14, no. 10, pp. 1479–1485, Oct. 2005.

[8] U. Ghanekar, A. K. Singh, and R. Pandey, "A contrast enhancement-based filter for removal of random valued impulse noise," IEEE Signal Process. Lett., vol. 17, no. 1, pp. 47–50, Jan. 2010.

[9] Y. wan, Q Chen and Y. Yang, "Robust impulse noise variance estimation based on image histogram," IEEE Signal Process. Lett., vol. 17, no. 5, pp. 485–488, May. 2010.

[10] M. Kim and M. G. Chung, "Recursively separated and weighted histogram equalization for brightness preservation and contrast enhancement," IEEE Trans. Consumer Electron., vol. 54, no. 3, pp.1389–1397, Aug. 2008.